J. Fluid Mech. (2008), *vol.* 603, *pp.* 463–473. © 2008 Cambridge University Press
doi:10.1017/S0022112008001195 Printed in the United Kingdom

Unsteady shock wave dynamics

P. J. K. BRUCE AND H. BABINSKY

Department of Engineering, University of Cambridge, Trumpington Street, Cambridge CB2 1PZ, UK

(Received 7 December 2007 and in revised form 4 March 2008)

An experimental study of an oscillating normal shock wave subject to unsteady periodic forcing in a parallel-walled duct has been conducted. Measurements of the pressure rise across the shock have been taken and the dynamics of unsteady shock motion have been analysed from high-speed schlieren video (available with the online version of the paper). A simple analytical and computational study has also been completed. It was found that the shock motion caused by variations in back pressure can be predicted with a simple theoretical model. A non-dimensional relationship between the amplitude and frequency of shock motion in a diverging duct is outlined, based on the concept of a critical frequency relating the relative importance of geometry and disturbance frequency for shock dynamics. The effects of viscosity on the dynamics of unsteady shock motion were found to be small in the present study, but it is anticipated that the model will be less applicable in geometries where boundary layer separation is more severe. A movie is available with the online version of the paper.

1. Introduction

The dynamic response of shock waves to unsteady perturbations in flow properties is a complex phenomenon. Current understanding has not yet reached the level where unsteady shock motion can be predicted reliably. The phenomenon is especially relevant to the behaviour of transonic shocks, which are sensitive to both upstream and downstream flow conditions. Changes in the flow properties ahead or downstream of a transonic shock can lead to shock motion. The exact nature of this motion is thought to depend on a combination of inviscid and viscous factors including the amplitude and frequency of the disturbance and the presence of boundary layers or regions of flow separation. The mechanism by which disturbances propagate through the flow to reach and influence the shock is also of interest for understanding the physics of unsteady shock motion.

The large changes in local flow properties across shock waves mean that unsteady shock motion can lead to large undesirable local fluctuations in properties such as shear stress, pressure and the rate of heat transfer. For this reason, large-amplitude unsteady motion is of most concern in aerodynamic applications. Examples include buffet on transonic aerofoils and engine unstart in supersonic engine intakes, both of which can be caused by periodic pressure perturbations generated downstream of the shock. In a study of transonic buffet, Lee (2001) concluded that pressure perturbations originating in an aerofoil's wake play a key role in shock unsteadiness, while Seddon & Goldsmith (1999) state that engine unstart can be caused by disturbances generated at the face of a downstream compressor. In contrast, studies exploring the relationship between shock unsteadiness and upstream disturbances in the incoming flow have

https://doi.org/10.1017/S0022112008001195 Published online by Cambridge University Press

reported that the resulting unsteady shock motion is commonly of a much higher frequency and smaller scale, making it of less concern for aerodynamic applications. Adam & Schnerr (1997) also report that oscillatory shock motion can be triggered by phase transition in two-phase flows.

Some experimental and numerical studies have been carried out using a variable-geometry second throat to investigate the effects of downstream periodic pressure perturbations on shocks (see for example Sajben & Kroutil 1981; Ott, Bolcs & Fransson 1995; Handa, Masuda & Matsuo 2003; Bur *et al.* 2006). All have reported that the amplitude of shock oscillation decreases with increasing perturbation frequency, although the reasons for this are not discussed in detail. In all of these studies, the shock is located in a duct of varying cross-sectional area, which complicates the flow field and makes it difficult to differentiate between effects that are truly unsteady and those that are due to geometry. This is well illustrated in the study of Bur *et al.* (2006), where large changes in shock strength and extent of boundary layer separation occur as the shock changes position on the downstream side of a bump, making it hard to identify more subtle unsteady effects.

One exception is a study by Edwards & Squire (1993), who investigated unsteady shock behaviour in a duct with parallel walls. They reported that shock amplitude was inversely proportional to frequency and that the pressure rise through an unsteady shock was linked to the relative Mach number ahead of the shock. Their findings suggest that much can be learned about unsteady shock dynamics by considering a shock in a parallel-walled duct where the upstream Mach number does not vary with shock position. This is the basis for the current work, which looks at the response to downstream periodic forcing of a normal shock in a parallel-walled duct.

In the present study, detailed information on shock dynamics and also the structure of the unsteady shock/boundary layer interaction (SBLI) have been obtained from high-speed schlieren images of the flow. The aim was to identify the key mechanisms that govern unsteady shock dynamics, such as how information is transmitted from the perturbation source to the shock and also the relative importance of viscous and inviscid effects. Experiments by Atkin & Squire (1992) in the experimental facility used here have shown that incipient shock-induced boundary layer separation occurs with a free-stream Mach number ahead of the shock of 1.4, while a more fully developed separated interaction exists at Mach 1.5. Tests have been conducted at both of these Mach numbers to study the effect of boundary layer separation on shock dynamics. It is hoped that the work will improve current understanding of unsteady shock motion to the level where it can be reliably predicted and controlled.

2. Experimental study

2.1. *Methods*

Experiments have been performed in the blowdown-type supersonic wind tunnel of the University of Cambridge. The tunnel has a rectangular working section with a constant cross-section 114 mm wide by 178 mm high. In the absence of a shock, the streamwise pressure gradient in the tunnel is extremely small and streamwise changes in the properties of the naturally grown tunnel wall boundary layer along the working section are negligible. An elliptical cam was mounted in the first diffuser, 790 mm downstream of the centre of the viewing window to create a variable second throat, as shown in figure 1. During runs, the tunnel stagnation pressure was held constant and the cam was rotated at frequencies between 8 and 45 Hz to produce an almost sinusoidal periodic variation in tunnel back pressure at a frequency double

https://doi.org/10.1017/S0022112008001195 Published online by Cambridge University Press

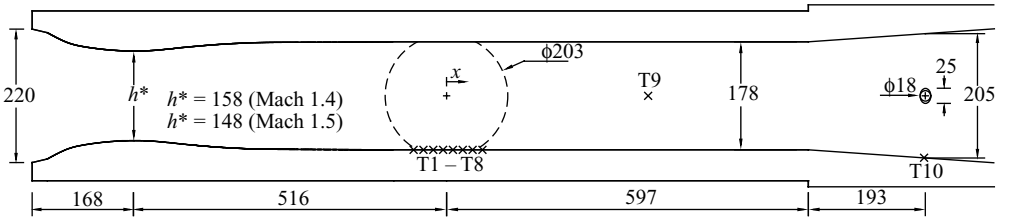


FIGURE 1. Experimental arrangement. The area of optical access is shown as a dashed circle. The reference location $x = 0$ is defined as the centre of this circle. Transducer locations are shown as crosses labelled T1 to T10. All dimensions are in mm.

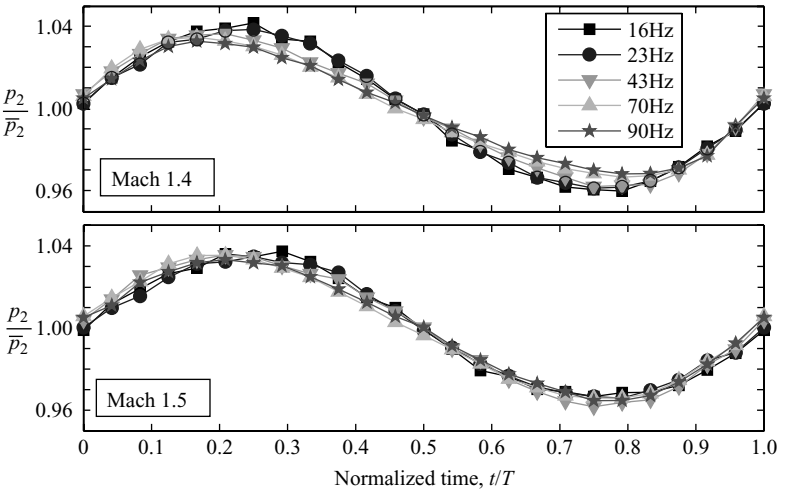


FIGURE 2. Variation of downstream pressure, p_2, due to rotation of the elliptical cam. Plotted profiles show the cycle-averaged variation based on a large number of complete cycles.

that of cam rotation. Preliminary tests revealed problems with resonance effects at some frequencies and results are only presented for five frequencies that were found to exhibit no resonant behaviour. The tunnel operating parameters were chosen such that the shock was located at the centre of the working section window under steady flow conditions. The working fluid in the tunnel is air and tests were carried out with an upstream stagnation pressure of 140 kPa and stagnation temperature of 290 K.

The cycle-averaged variation of downstream pressure measured at transducer T9 ($x = 330$ mm) for the range of cam rotational frequencies is plotted in figure 2. This fluctuating back pressure caused the position of the tunnel's normal recovery shock to oscillate about a mean position. The pressure profiles shown in figure 2 are very similar for both Mach numbers and vary only slightly with frequency. There is a slight trend of decreasing pressure perturbation amplitude with increasing frequency in the Mach 1.4 case of the order of 10% for the frequencies tested. The slight skewness of the profiles at high frequencies is due to bunching and spreading of compression and expansion waves as they travel upstream from the cam (where they are generated) to the shock.

The eight pressure transducers labelled T1 to T8 in figure 1 were located directly beneath 0.5 mm diameter holes in the tunnel floor, covering the streamwise range

https://doi.org/10.1017/S0022112008001195 Published online by Cambridge University Press

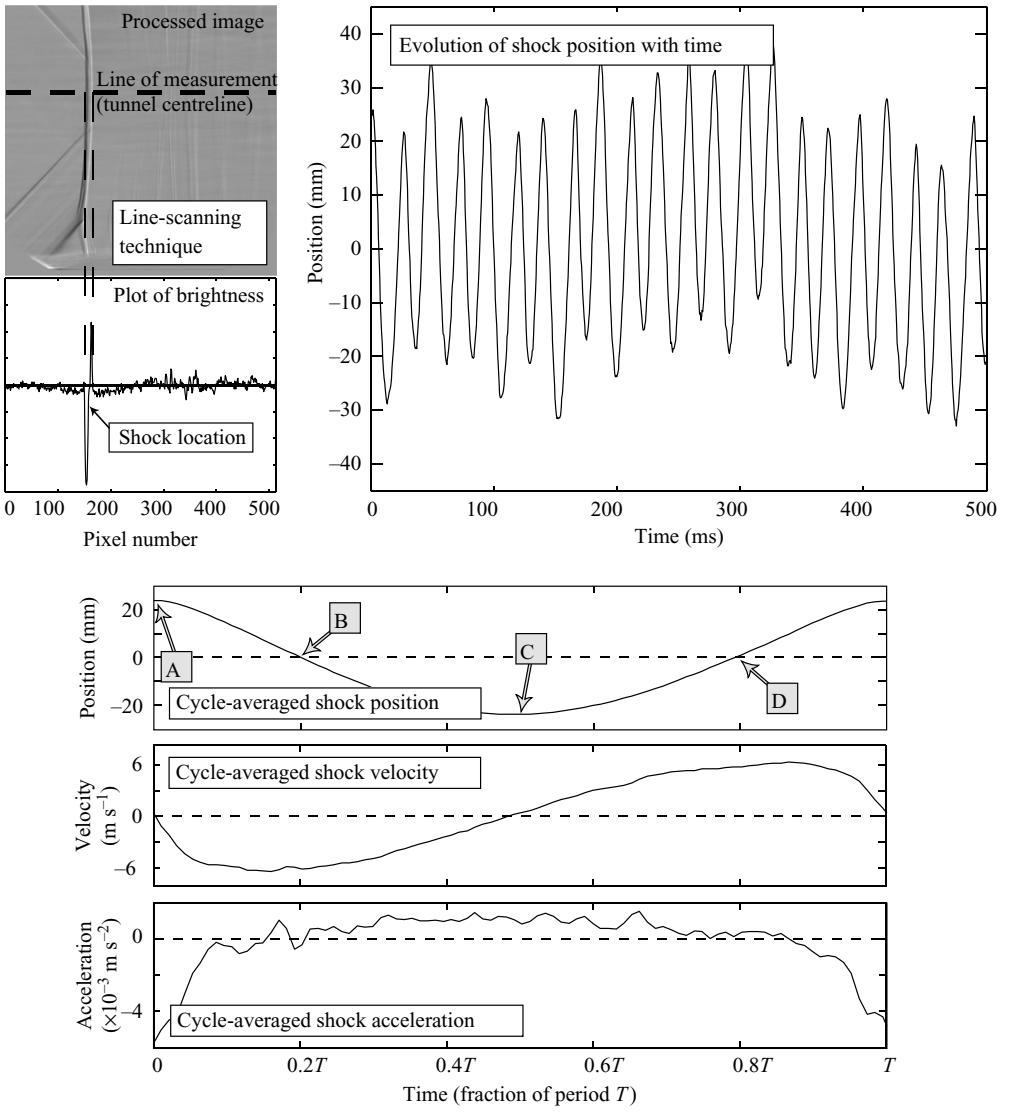


FIGURE 3. Method for tracking shock position with time. Images and data shown are for $M_\infty = 1.4$ with a shock oscillation frequency of 43 Hz. The labels A–D correspond to the images shown in figure 4.

$-65 \leqslant x \leqslant 65$ mm. A sampling rate of 4 kHz was used to capture sufficient data for the calculation of reliable mean values. The free-stream velocity was approximately 410 m s^{-1} at Mach 1.4 and 430 m s^{-1} at Mach 1.5. High-speed schlieren images were obtained using a Photron FASTCAM-ultima APX high-speed camera at a frame rate of 6 kHz and 512 × 512 pixel resolution. Images presented here have been cropped and processed to remove noise due to irregular camera pixel sensitivity. Figure 3 outlines the method used to obtain information on shock dynamics from high-speed video footage. A line-scanning technique was developed to determine shock position in each frame with an accuracy based on pixel size of better than 0.5 mm. This is of the order of 1% of the shock's amplitude of motion. For each test case, several

https://doi.org/10.1017/S0022112008001195 Published online by Cambridge University Press

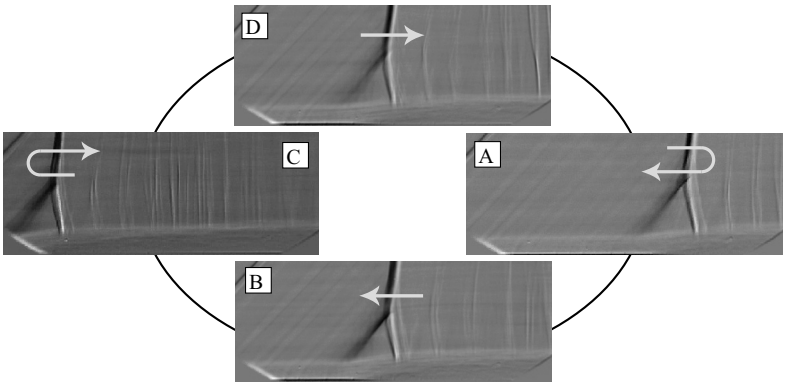


FIGURE 4. Schlieren images for a shock wave oscillation frequency of 43 Hz at $M_\infty = 1.4$. Images measure 110 mm by 40 mm. Arrows indicate the direction of shock motion. A movie is available with the online version of the paper.

seconds of periodic motion were recorded and processed to produce a plot of mean shock position throughout a cycle. Information on shock velocity and acceleration was then obtained by differentiation of this profile.

Figure 3 shows that the mean position of the shock undergoes irregular low-frequency 'wandering' by up to ± 20 mm due to tunnel operator error. This has a negligible impact on results due to the parallel walled geometry of the working section and the very low frequency at which the irregular shock 'wandering' occurs. The 'wandering' was taken advantage of to increase the resolution and range of pressure measurements in the interaction region, using a technique previously developed by Atkin & Squire (1992).

2.2. *The interaction structure between an unsteady shock and a turbulent boundary layer*

When subjected to sinusoidal variations of downstream pressure, the normal shock undergoes consistent and repeatable periodic motion, as seen in figure 3. Throughout this periodic motion, the structure of the SBLI varies slightly. Figure 4 shows a selection of schlieren images that correspond to the points in the cycle marked A, B, C and D in figure 3. The images show a subtle difference between the structure during upstream (B) and downstream (D) motion. The well-defined leading leg of the lambda shock foot structure seen during upstream motion (B) becomes much fainter and almost disappears during downstream motion (D). Downstream of the main shock, additional weak shocks can be seen, suggesting significant post-shock re-acceleration of the flow and the presence of secondary supersonic regions.

In a study of steady normal shocks of different strengths in the same experimental facility, Atkin & Squire (1992) reported that at $M_\infty = 1.4$, a weak lambda shock foot structure, that was not present at lower Mach numbers, first appeared. This change of structure is associated with the onset of shock-induced boundary layer separation. Hence it can be concluded that the changes in SBLI structure observed in figure 4 are related to variations in the extent of shock-induced boundary layer separation. These variations are due to changes in the *relative* strength of the shock and hence pressure rise as the shock moves upstream and downstream. The schlieren images show some evidence supporting this theory, although the exact extent of boundary layer separation is not clear. The angle of the leading shock leg and the overall size of the interaction are also different during upstream and downstream shock motion.

https://doi.org/10.1017/S0022112008001195 Published online by Cambridge University Press

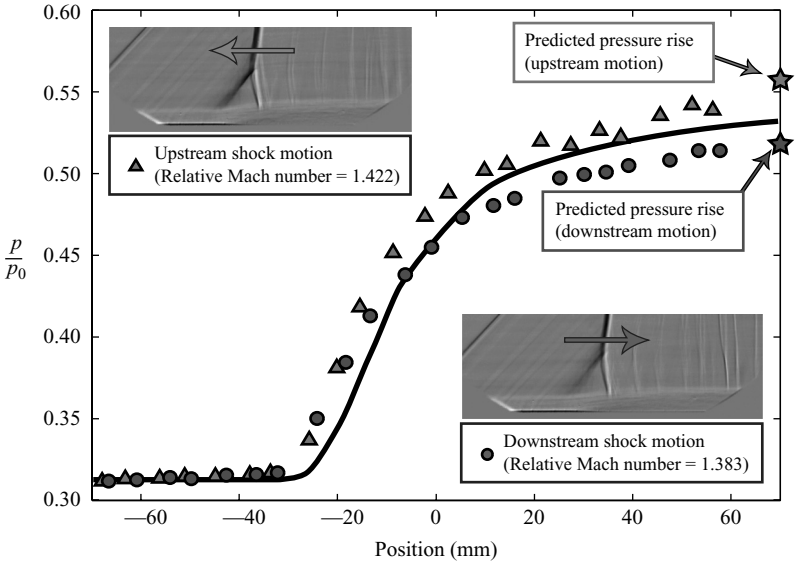


FIGURE 5. Comparison of pressure rise during upstream and downstream shock wave motion for $M_\infty = 1.4$ with a shock wave oscillation frequency of 70 Hz. The pressure rise across the steady interaction is shown as a solid line for comparison.

No significant variations in SBLI structure were observed at $M_\infty = 1.5$, where the pressure ratio remained large enough to separate the boundary layer during both upstream and downstream shock motion.

The shape and magnitude of the pressure rise across the unsteady shock also varies during an oscillation. The pressure rise at two points of the unsteady cycle when the shock wave is in the same place but travelling in different directions (points B and D in figure 4) is plotted in figure 5. The pressure rise through a steady Mach 1.4 shock was also measured and is shown for comparison. Also marked on the graph are two predicted downstream pressures and these are discussed in the following section.

2.3. *Unsteady shock dynamics*

Figure 5 shows that the pressure rise through the shock is larger during upstream motion than during downstream motion. This can be explained by changes in the relative Mach number ahead of the shock. From figure 3, the peak shock velocity during unsteady motion at $M_\infty = 1.4$ and 43 Hz is around 6 m s^{-1} in both directions, which is approximately 1.5% of the free-stream velocity. This causes the relative Mach number ahead of the shock to vary by an equivalent amount, as indicated in figure 5. The two predicted downstream pressures plotted in figure 5 were calculated based on the expected pressure rise across a steady interaction at the instantaneous relative Mach numbers shown on the images.

The predicted pressure rises closely match the experimental data in figure 5, supporting the idea that the magnitude of the pressure jump across an unsteady shock depends primarily on the relative Mach number ahead of the shock. From this, it can be concluded that the mechanism by which the shock responds to back pressure variations is to move so that its relative Mach number matches the imposed pressure jump. The changes in relative Mach number are also responsible for the observed changes in lambda shock foot structure seen in figure 4. Although the variations in relative Mach number are small, they have a significant effect on the interaction

https://doi.org/10.1017/S0022112008001195 Published online by Cambridge University Press

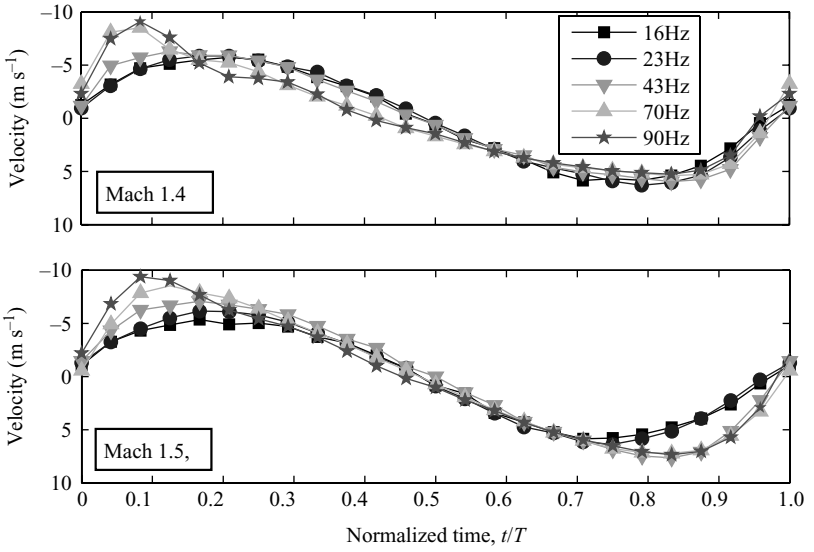


FIGURE 6. Effect of frequency on shock velocity at Mach 1.4 and 1.5. Note that velocity is plotted inverted to aid comparison with the pressure plots in figure 2.

structure because the extent of shock-induced separation is very sensitive to changes in shock strength at this Mach number.

The above analysis suggests that unsteady shock behaviour is different to the classical steady case where a shock in a diverging duct responds to a step change in back pressure by changing its position to one with increased or decreased duct area to increase or decrease its absolute (rather than relative) strength. This explains why it is possible to produce oscillatory shock motion in a duct with parallel walls, where a step change in back pressure would cause the shock to move out of the tunnel working section and into the nozzle or diffuser. Furthermore, it follows that the velocity of shock motion should only depend on the imposed pressure ratio and should be independent of perturbation frequency providing the amplitude of downstream pressure perturbation is also independent of frequency, as is the case here (see figure 2). Plots of cycle-averaged shock velocity for the range of frequencies tested at $M_\infty = 1.4$ and 1.5 are shown in figure 6.

The results show that shock velocity is indeed approximately independent of frequency for most of the period. The implications of this for the amplitude–frequency relation of an oscillating shock in a duct are considered in the analytical and computational study described in § 3. Figure 6 does suggest that some frequency-dependent behaviour exists in the first part of the cycle, although these effects are not considered to significantly affect the amplitude of shock motion and are not considered in this paper. It is likely that the frequency-dependent behaviour is related to viscous effects triggered by the acceleration spike seen at the start of the cycle in figure 3.

3. Analytical and computational study

In addition to experiments, a simple analytical and computational study of a normal shock in a duct subject to downstream pressure variations has been conducted. Parallel and diverging duct geometries have been investigated, as shown in figure 7.

https://doi.org/10.1017/S0022112008001195 Published online by Cambridge University Press

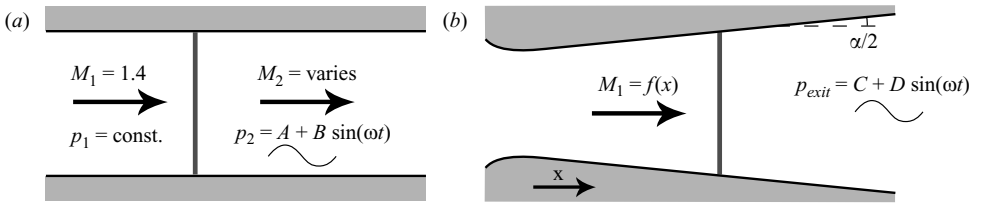


FIGURE 7. Duct geometries used for the analytical and computational study: (*a*) parallel walls, (*b*) diverging walls.

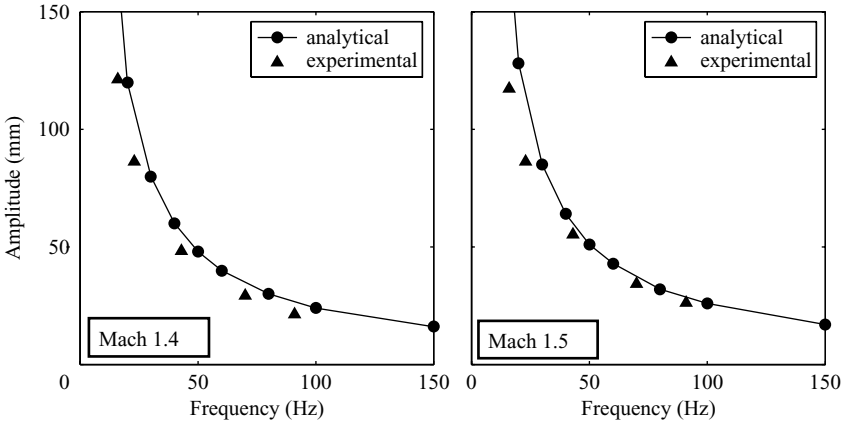


FIGURE 8. Variation of amplitude with frequency in a duct with parallel walls. Comparison of analytical and experimental results.

The amplitude of the pressure variation immediately downstream of the shock was set to be 4% of the mean downstream pressure to match experimentally measured values (see figure 2). The absolute value of the mean downstream pressure was set to the inviscid post-shock value in a parallel duct and to the value that gave the required mean shock position and strength in the diverging duct.

In the analytical study, the flow was assumed to be quasi-steady. Based on this assumption, the relative shock strength required to satisfy the imposed varying pressure ratio was calculated from the Rankine–Hugoniot equation as a function of time. For a duct with parallel walls, the shock velocity was then calculated and integrated to give the shock trajectory and thus the amplitude of unsteady shock motion. Calculated amplitudes at Mach 1.4 and 1.5 over a range of pressure fluctuation frequencies are shown in figure 8, together with experimentally measured amplitudes.

The agreement between prediction and experiment is very good with experimentally measured amplitudes typically within 10% of the analytical predictions. Experimentally measured shock oscillations were slightly larger at Mach 1.5 than at 1.4 and this was also the case in the analytical results. Significantly, these results suggest that an inviscid quasi-steady one-dimensional model makes reasonable predictions of shock dynamics even in cases with significant viscous and two-dimensional effects.

Figure 8 predicts that oscillation amplitudes become infinitely large for frequencies tending to zero. While this is correct for an inviscid parallel-walled duct, it cannot be the case in a diverging duct, where the gas state ahead of the shock varies with streamwise position and causes the amplitude to remain finite as the frequency

https://doi.org/10.1017/S0022112008001195 Published online by Cambridge University Press

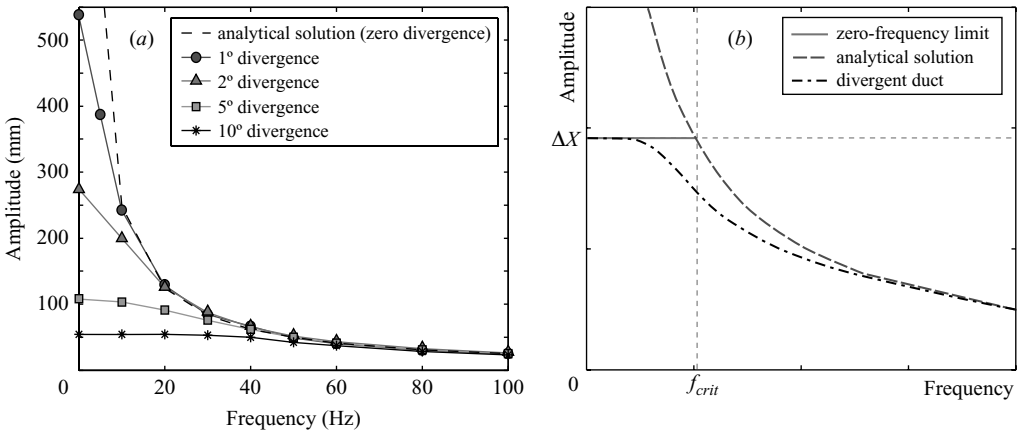


FIGURE 9. Amplitude–frequency relation in a diverging duct (*a*) Computational and analytical results for $M = 1.4$, (*b*) general amplitude–frequency relation.

tends to zero. The effect of divergence has been studied here computationally using a simple one-dimensional Euler scheme and the results for a selection of duct divergence angles, all with a steady shock strength of Mach 1.4 and the same downstream pressure perturbation amplitude, are presented in figure 9(*a*). This technique of perturbing the Euler equations was used by MacMartin (2004) to study the dynamics of a transonic shock in an engine intake and enabled him to develop a simple feedback-control system for shock instability based on the detection of shock position.

The results in figure 9(*a*) show that at low frequency, the amplitudes of shock motion tend to limit values, which correspond to the difference in the steady shock positions at the extremes of the duct exit pressures. These effectively set the 'steady state' upstream and downstream positions of the shock and hence the 'zero-frequency amplitude'. At higher frequencies, the amplitude of shock oscillation is largely independent of divergence angle and very closely matches the analytical prediction for parallel ducts. This suggests that the dynamics of shock oscillations can be split into two domains: one at low frequency where the oscillation amplitude is primarily determined by geometric factors, and one at high frequencies where the behaviour becomes independent of geometry.

4. Amplitude–frequency relation in a diverging duct

For a periodically varying downstream pressure in a given divergent geometry, a critical frequency of pressure perturbation, f_{crit}, exists such that: at frequencies below f_{crit}, the amplitude of shock motion tends to the steady-state amplitude ΔX, which is determined by the divergence of the duct and is independent of frequency, while at frequencies above f_{crit}, the amplitude becomes almost independent of duct divergence and is only a function of frequency. The situation for a given geometry and pressure perturbation amplitude is shown schematically in figure 9(*b*).

This two-domain model has been extended into a design tool for the assessment of shock stability with the use of dimensional analysis. The non-dimensional amplitude and frequency from a range of simulations, including those shown in figure 9 and also experimental results from Bur *et al.* (2006), are plotted in non-dimensional form in figure 10. Scaling variables were chosen to match zero-frequency amplitudes between tests at different conditions. The results collapse onto one line with reasonable

https://doi.org/10.1017/S0022112008001195 Published online by Cambridge University Press

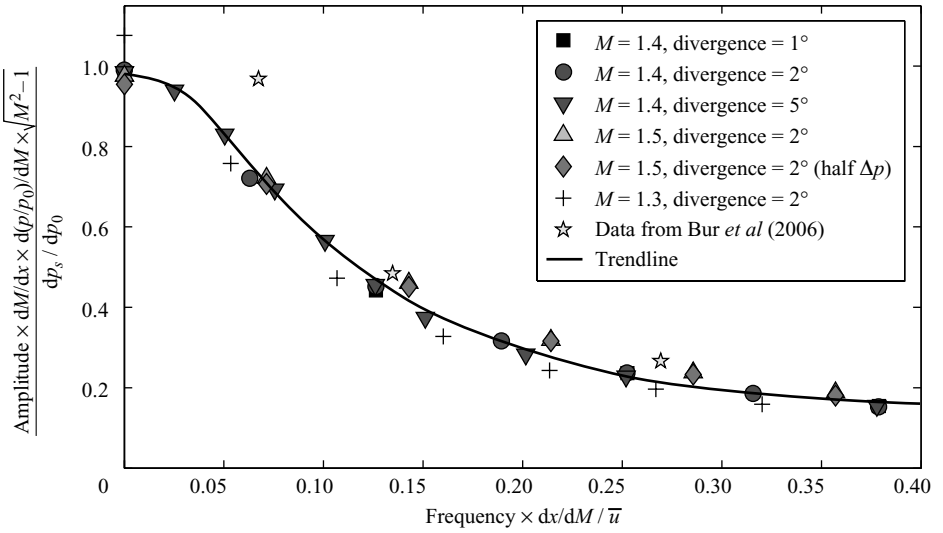


FIGURE 10. Non-dimensional amplitude–frequency relation in a diverging duct. $\mathrm{d}M/\mathrm{d}x$ is the local-Mach-number gradient determined at the mean shock position, $d(p_s/p_0)$ is the amplitude of post-shock pressure variation normalized by the upstream stagnation pressure and $\bar{u}$ is the free-stream velocity upstream of the shock.

agreement for the range of Mach numbers and duct geometries shown, supporting the choice of non-dimensional scaling variables. The non-dimensional zero-frequency amplitude is approximately 1 and the critical frequency, as defined in figure 9(*b*), is around 0.04.

The non-dimensional relationship encapsulated in figure 10 allows the relative importance of geometry to be assessed in applications where unsteady shocks occur. In applications where information is available on the magnitude and frequency of expected downstream pressure perturbations, it enables designers to determine whether shock stability is affected by geometry and, in cases where it is, provides a basis for developing designs that mitigate undesirable unsteady effects. The model is not limited to shocks in diverging ducts and could be used in other applications such as transonic aerofoils and turbomachinery where data on the variation of Mach number with aerofoil or blade chord ($\mathrm{d}M/\mathrm{d}x$) is available from steady experiments or simulations. The model also provides a method for the prediction of shock oscillation amplitudes in existing applications with shock instability problems. In these cases, the magnitude of pressure perturbation required to produce a critical oscillation amplitude could be predicted and used as part of a feedback control system to prevent phenomena such as buffet or engine unstart.

The validity of the model is expected to be poor when severe boundary layer separation occurs, such as applications with very strong shocks or large duct divergence angles. The frequency-dependent behaviour identified in figure 6 is not thought to be of concern as oscillation amplitudes are small as the effects become noticeable at high frequency. Although this suggests viscosity does not matter, it is widely accepted that the upstream propagation of pressure information in the boundary layer has a key role in unsteady shock dynamics (see for example Lee 2001; Bur *et al.* 2006) and so it is more likely that the model developed here simply fails to capture the full physics of the flow.

https://doi.org/10.1017/S0022112008001195 Published online by Cambridge University Press

5. Conclusions

Experiments on the dynamics of unsteady shock motion have been performed. Normal shocks have been observed to undergo oscillatory motion in response to an imposed varying pressure ratio. It is concluded that the mechanism by which shocks respond to back pressure variations is to change their relative strength by moving so that their relative Mach number matches the pressure jump. These changes in relative shock strength can lead to changes in the extent of boundary layer separation and SBLI structure.

The dynamics of unsteady shock motion measured in experiments have been reproduced by a simple inviscid analytical model. A relationship between the amplitude and frequency of shock motion in a diverging duct has been outlined, based on the concept of a critical frequency that relates the relative importance of geometry and disturbance frequency on shock dynamics. A non-dimensional version has been found that allows the amplitude of shock oscillation in response to a known pressure perturbation to be predicted and enables the relative importance of geometry in an application to be assessed.

The present research is funded through the E.U. project UFAST.

REFERENCES

Adam, S. & Schnerr, G. H. 1997 Instabilities and bifurcation of non-equilibrium two-phase flows. *J. Fluid Mech.* **348**, 1–28.

Atkin, C. J. & Squire, L. C. 1992 A study of the interaction of a normal shock wave with a turbulent boundary layer at Mach numbers between 1.30 and 1.55. *Eur. J. Mech.* **11**, 93–118.

Bur, R., Benay, R., Galli, A. & Berthouze, P. 2006 Experimental and numerical study of forced shock-wave oscillations in a transonic channel. *Aerospace Sci. Techn.* **10**, 265–278.

Edwards, J. A. & Squire, L. C. 1993 An experimental study of the interaction of an unsteady shock with a turbulent boundary layer at mach numbers of 1.3 and 1.5. *Aero. J.* **97**, 337–348.

Handa, T., Masuda, M. & Matsuo, K. 2003 Mechanism of shock wave oscillation in transonic diffusers. *AIAA J.* **41**, 64–70.

Lee, B. H. K. 2001 Self-sustained shock oscillations on airfoils at transonic speeds. *Prog. Aerospace Sci.* **37**, 147–196.

MacMartin, D. G. 2004 Dynamics and control of shock motion in a near-isentropic inlet. *J. Aircraft* **41**, 846–853.

Ott, P., Bolcs, A. & Fransson, T. H. 1995 Experimental and numerical study of the time-dependent pressure response of a shock wave oscillating in a nozzle. *J. Turbomachinery* **117**, 106–114.

Sajben, M. & Kroutil, J. C. 1981 Effects of initial boundary layer thickness on transonic diffuser flows. *AIAA J.* **19**, 1386–1393.

Seddon, J. & Goldsmith, E. L. 1999 *Intake Aerodynamics*, 2nd edn. AIAA.

https://doi.org/10.1017/S0022112008001195 Published online by Cambridge University Press